Unified Scaling of Network Strength in Cellulose Nanofibrils from Dilute Suspensions to Dense Mats

Jaeho Ryu [a], and Hye Jung Youn [b,c,*]

While the rheological properties of low-consistency cellulose nanofibril (CNF) suspensions and the mechanical properties of dry CNF films have been reported, research on high-consistency suspensions and wet CNF mats remains limited. Understanding suspension behavior during dewatering over a wide range of solids contents is essential. In this study, CNF consistency was controlled up to 20% using pressurized dewatering, and rheological behavior was characterized up to 10.2% solids content. Tensile testing was applied at higher concentrations where mat-like behavior emerged. The network strength followed a consistent power-law relationship across the entire solids content range, with a scaling exponent of 2.74, indicating that CNF flocculation is fundamentally similar to that of pulp fiber behavior despite its higher aspect ratio and smaller dimensions. CNF initiated network formation at a consistency more than twice as low as that of pulp fiber and exhibited a 5- to 20-fold higher network strength. At high solids contents, tensile strength increased exponentially, while elongation reached a maximum at approximately 50% solids content, suggesting a transition from capillary-driven consolidation to a hydrogen-bonded network. Nanofibrillation enhanced both tensile breaking stress and strain-at-break across all investigated solids contents. These results provide a framework for controlling CNF structural properties during dewatering and consolidation.

DOI: 10.15376/biores.21.3.6726-6740

Keywords: Cellulose nanofibril; High consistency; Mechanical properties; Rheological properties; Network strength

Contact information: a: R&D Center, Greeneple Inc., 21 Kentech-ro, Naju, 58330, Korea; b: Department of Agriculture, Forestry and Bioresources, College of Agriculture and Life Sciences, Seoul National University, 1, Gwanak-ro, Gwanak-gu, Seoul, 08826, Korea; c: Research Institute of Agriculture and Life Sciences, Seoul National University, 1, Gwanak-ro, Gwanak-gu, Seoul, 08826, Korea;
** Corresponding author: page94@snu.ac.kr*

INTRODUCTION

Cellulose nanofibrils (CNF), which are also called nanofibrillated cellulose, have attracted growing attention as high-performance and sustainable materials for a wide range of applications, including cosmetics, automotive components, pharmaceuticals, electronics, and papermaking. These diverse applications arise from the unique physical characteristics of CNF, particularly their high aspect ratio and hydrophilic surface chemistry, which enable the formation of robust, percolated networks even at very low solids contents. As a result, CNF suspensions exhibit distinctive rheological behaviors that make them versatile building blocks for advanced functional materials.

Extensive research has focused on elucidating the rheological properties of CNF suspensions at low solids contents, where network formation, entanglement, and

flocculation dominate material behavior (Tatsumi *et al.* 2002; Pääkkö *et al.* 2007; Agoda-Tandjawa *et al.* 2012). Tatsumi and Matsumoto (2007) demonstrated that the storage modulus of cellulose fiber suspensions follows a power-law relationship with consistency, with the exponent strongly influenced by fiber aspect ratio and flexibility. When expressed in terms of volume consistency, the power-law exponent approaches three, which is consistent with theoretical predictions and experimental observations for fiber suspensions (Bennington *et al.* 1990). Building on this framework, Pääkkö *et al.* (2007) applied rigid polymer network models (Jones and Marquès 1990) to CNF systems, showing that nanofibrils form highly entangled, three-dimensional networks that exhibit storage moduli orders of magnitude higher than those of cellulose nanocrystals. Hubbe *et al.* (2017) reviewed of the rheology of nanocellulose-rich suspensions, summarizing the effects of fiber morphology, network formation and breakup, wall slip, and colloidal factors on rheological behavior. Their review further summarized numerous studies reporting power-law relationships between solids concentration and rheological properties, including viscosity and yield points, and discussed the interpretation of rheological responses in highly structured nanocellulose systems.

Recent studies have further advanced the understanding of cellulose nanofibril systems by elucidating molecular-scale assembly mechanisms and functional properties. For example, Zhang *et al.* (2023a,b) investigated the structural organization and formation pathways of cellulose nanofibrils, while Ai *et al.* (2024) reported emerging functionalities of cellulose nanomaterials, including catalytic behavior and advanced material applications. In parallel, increasing efforts have been devoted to understanding the rheological behavior and network structure of CNF suspensions beyond conventional linear viscoelastic analysis. Recent studies have applied advanced rheological approaches, such as large amplitude oscillatory shear (LAOS), to capture nonlinear structural responses and network evolution in nanocellulose systems (Solhi *et al.* 2023; Xu *et al.* 2024). These approaches provide deeper insights into the relationship between microstructure and macroscopic mechanical behavior of fibrillar networks.

Beyond macroscopic rheology, the microstructural characteristics of CNF networks have been investigated using imaging techniques. Saarikoski *et al.* (2012) reported that the flocculated structures formed by CNF suspensions are remarkably similar to those observed in conventional pulp fiber suspensions, despite the nanometer-scale dimensions of CNF. This finding aligns with decades of research on fiber flocculation in papermaking systems (Beghello 1998; Wågberg and Nordqvist 1999; Björkman 2003a,b; Karppinen *et al.* 2012), suggesting that fundamental network principles may persist across length scales.

Since CNF originates from cellulose fibers, classical theories describing the suspension dynamics and network behavior of pulp fibers provide a valuable framework for understanding CNF systems, particularly at elevated solids contents. In papermaking, fiber dispersion and flocculation in the wet-end strongly influence sheet uniformity and final product quality (Björkman 2000; Kerekes 2006). Kerekes *et al.* (1985) identified three governing mechanisms for fiber network formation—colloidal aggregation, mechanical entanglement, and elastic bending—which collectively explain how increasing consistency enhances network strength but often compromises processability. Consistent with these concepts, the network strength of fiber suspensions has been shown to increase with consistency following a power-law relationship, with volume fraction playing a key role in determining network strength (Bennington *et al.* 1990; Youn and Lee 2002).

At higher solids contents, rheological behavior alone is insufficient to describe material performance, and mechanical integrity becomes a critical factor. The strength of

wet fiber mats, commonly referred to as wet web strength, governs runnability and stability during papermaking operations. Numerous studies have shown that wet web strength evolves with solids content and is controlled by different mechanisms across concentration regimes (Lyne and Gallay 1954; Seth *et al.* 1984; Page 1993; Seth 1995). At low solids contents, surface tension forces dominate network cohesion, whereas above approximately 40% solids content, direct fiber-to-fiber interactions become increasingly important (Seth *et al.* 1984). In this higher-solids regime, fiber morphology—particularly fiber length and coarseness—plays a decisive role in determining wet web strength, as fibers typically do not fracture during wet failure (Nordman *et al.* 1972; Seth 1990, 1995).

The mechanical properties of CNF in the form of dry films have also been widely studied. Reported tensile strengths range from approximately 80 to 300 MPa, with strains at break between 2.5% and 17.5%, depending on cellulose source and processing conditions (Zimmermann *et al.* 2004; Leitner *et al.* 2007; Siró and Plackett 2010). While theoretical models predict elastic moduli approaching tens of gigapascals for idealized fibrillar networks (Cox 1952; Page *et al.* 1977), experimentally measured values are substantially lower, reflecting deviations from ideal alignment, fibril straightness, and bonding efficiency.

Despite these advances, the continuous evolution of CNF network properties during the transition from dilute suspension to highly consolidated wet mat remains poorly understood. Recent studies have begun to explore the rheology of nanocellulose systems at higher solids contents, emphasizing the roles of yield stress and thixotropy in network development (Solhi *et al.* 2023; Xu *et al.* 2024). However, a unified description that spans the full solids content range—from dilute suspensions to nearly dry CNF mats—is still lacking. This gap arises largely from the practical challenges associated with dewatering CNF, as the nanometer-scale dimensions and high specific filtration resistance severely limit the applicability of conventional water removal techniques.

Therefore, the objective of this study is to investigate the rheological and mechanical properties of CNF networks across an exceptionally broad range of solids contents, from 0.5% to 99%. By employing pressurized dewatering to control consistency up to 20%, followed by controlled drying at higher solids levels, this work examines whether the fundamental power-law relationship between network strength and solids content—well established for pulp fiber suspensions—remains valid for nanofibrillated cellulose throughout this structural transition. Furthermore, the influence of nanofibrillation intensity on network integrity is systematically evaluated, providing a unified framework that bridges classical fiber suspension theory and the behavior of nanoscale cellulose networks.

EXPERIMENTAL

Materials

Bleached *Eucalyptus* kraft pulp was used as the raw material for nanofibrillation. The length-weighted average fiber length, measured using a Kajaani FiberLab analyzer (KajaaniFiberLab V.3, Metso, Finland), was 0.51 mm. The chemical composition of the pulp fiber was determined according to the TAPPI method (T 203 om-93), revealing an α-cellulose content of 88.1% ± 1.1% and a hemicellulose content of 11.9% ± 1.1%.

Preparation of Nanocellulose

The CNF was prepared from the pulp fiber through mechanical treatment. As a pretreatment the pulp fiber was beaten to a freeness of 450 mL CSF using a laboratory Hollander (Valley) beater. The beaten pulp was then diluted to a solids content of 2 wt% and subjected to nanofibrillation using a grinder (Super Masscolloider, Masuko Sangyo Co., Japan), operated at a gap setting of −50 μm, and processed through multiple passes (0–15 passes) to control the degree of nanofibrillation.

The morphology of the samples was examined by FE-SEM (SUPRA 55VP, Carl Zeiss, Germany) and TEM (JEM1010, JEOL, Japan). For the FE-SEM analysis, the samples were coated with a thin conductive layer of Pt with a thickness of approximately 3 nm prior to imaging. The accelerating voltage was set to 2 kV, and the working distance was maintained between 2 and 4 mm. For TEM analysis, a dilute CNF suspension was prepared and a small droplet was deposited onto a carbon-coated copper grid. After allowing the sample to adsorb for several minutes, excess liquid was carefully removed using filter paper. The sample was subsequently negatively stained with uranyl acetate to enhance contrast of the fibrillar structure, and then air-dried prior to observation. TEM was operated at an accelerating voltage of 80 kV. Quantitative analysis of fibril width was conducted using ImageJ based on the TEM images, with measurements performed on more than 200 fibrils to ensure statistical reliability.

Preparation of CNF Mats with Varying Solids Contents

CNF suspensions with an initial consistency of 2% were dewatered using pressurized dewatering equipment (PDE, Quro, Korea). For samples with solids contents below 20%, the solids content was precisely controlled by adjusting the dewatering time under constant pressure. To obtain samples with solids contents above 20%, additional water removal was achieved by controlled air-drying at room temperature. As the solids content increased, the material progressively lost flowability and transitioned from a suspension to a gel-like state and ultimately to a wet mat. Each sample at elevated solids content was sealed and stored for a sufficient period to allow equilibration of moisture distribution throughout the CNF network. All CNF mats were prepared with an identical dry fiber basis weight of 200 g/m², regardless of solids content.

Characterization of Rheological Properties

The rheological properties of CNF were characterized using an Advanced Rheometric Expansion System (ARES, TA Instruments, USA) equipped with a parallel-plate geometry (ϕ = 25 mm). To ensure sufficient sensitivity to the CNF network structure, the gap between the plates was set in the range of 1 to 3 mm, and each sample was allowed to equilibrate for 5 min prior to measurement. Strain sweep tests were conducted at a constant frequency of 1 Hz (6.28 rad/s). During the strain sweep, the storage modulus (G') initially remained constant within the linear viscoelastic region and subsequently decreased as the network structure began to break down. The critical strain was determined as the intersection point of two tangents drawn to the plateau region of G' at low strain and the decreasing region at higher strain. The yield stress was then defined as the stress corresponding to this critical strain. Frequency sweep measurements were subsequently performed over a frequency range of 1 to 100 Hz at a constant strain of 1%, which was selected to remain within the linear viscoelastic region. During these measurements, the storage modulus (G'), loss modulus (G''), and complex viscosity were recorded.

Evaluation of Mechanical Properties of CNF Mats

The tensile properties of the CNF mat were evaluated using a Universal Testing Machine (UTM; Instron, USA) at a constant strain rate of 10%/min. Specimens with a width of 15 mm were prepared from CNF mats with varying solids contents. The span length between the clamps was 20 mm. The thickness of the specimens was measured as 0.3 to 1.3 mm for wet mats and approximately 0.2 mm for dry mats.

RESULTS AND DISCUSSION

Morphological Characterization of CNF

The morphological change of fibers during the nanofibrillation process was investigated using FE-SEM and TEM, as shown in Fig. 1. Figures 1(a–c) show FE-SEM images of the beaten fiber and CNFs at different grinding stages. Figure 1(a) shows the morphology of the beaten fiber prior to grinding, where the fibrous structure can be observed. After 5 passes (Fig. 1(b)), fibrillation had increased, indicating fiber delamination, while after 10 passes (Fig. 1(c)), the fibers were further fibrillated and fragmented into smaller elements. Although nanoscale fibrils cannot be directly resolved at this magnification, the overall reduction in fiber dimensions is evident.

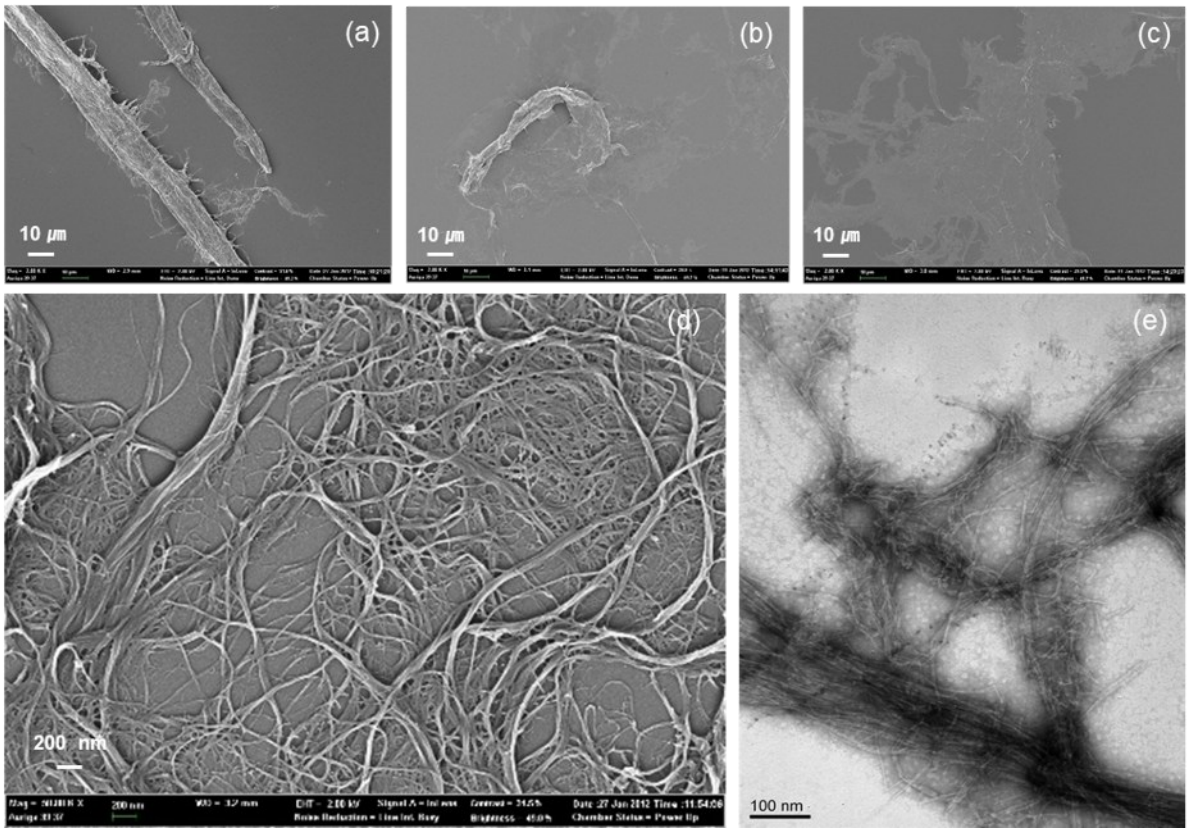

Fig. 1. Morphological evolution of cellulose fibers during the nanofibrillation process. (a) Beaten fiber prior to grinding, (b) CNF after 5 passes, (c) CNF after 10 passes, (d) CNF after 15 passes (high-magnification FE-SEM image), (e) TEM image of CNF after 15 passes; FE-SEM images in (a–c) were acquired at a magnification of ~2000×, while (d) was obtained at ~50,000×. The TEM image in (e) was acquired at ~200,000×.

A high-magnification image of the CNF after 15 passes is shown in Fig. 1(d). It reveals a heterogeneous network consisting of both individual nanofibrils and aggregated fibrillar structures, indicating an advanced stage of fibrillation. To further confirm the formation of nanoscale fibrillar elements, TEM analysis was performed for the 15-pass CNF (Fig. 1(e)). Due to the hierarchical structure of pulp fibers, the measured fibril width may vary depending on whether individual fibrils or fibril bundles are selected. However, for the CNF produced after 15 passes of grinding in this study, the average (mean) value of the CNF was approximately 15 nm, and the median value was approximately 10 nm. These results confirm that repeated grinding effectively produced nanoscale fibrillar structures.

Rheological Network Properties of CNF at Low to Intermediate Solids Contents

Rheological properties, such as storage modulus (G') and yield stress, characterize the network strength of CNF suspensions and have been reported in various studies (Tatsumi *et al.* 2002; Pääkkö *et al.* 2007; Agoda-Tandjawa *et al.* 2012). While these properties typically follow a power-law relationship with consistency, most experimental data have been limited to low solids contents, reaching only up to approximately 5.8% (Pääkkö *et al.* 2007). The power-law exponent is generally reported to be close to 3, whereas Agoda-Tandjawa *et al.* (2012) reported a slightly lower value of 2.58. Despite these theoretical foundations, characterization of CNF suspensions at higher solids contents remains challenging, as the rapidly increasing network stiffness often leads to unreliable dynamic measurements due to wall slip in parallel-plate geometries. By employing a controlled sample preparation and equilibration procedure prior to rheological testing, reliable measurements were obtained for CNF suspensions with solids contents of up to 10.2%.

Figure 2(a) presents the yield stress and critical strain of CNF, prepared by 15 passes through the grinder, as a function of solids content up to 10.2%. Yield stress is widely accepted as a direct measure of network strength (Kurath 1959; Bennington *et al*. 1990; Kerekes and Schell 1992; Tatsumi *et al*. 2002). The results show that as solids content increases, the network strength significantly enhances. Conversely, the critical strain — the point distinguishing the linear and non-linear viscoelastic regions, which indicates the onset of nanofibril network breakdown — decreases with increasing solids content. This inverse relationship indicates that the CNF network becomes increasingly rigid as it densifies. However, for samples exceeding 10% solids content, dynamic measurements using parallel plate geometry became unreliable due to the increased stiffness of the mat-like structure and potential slip between the plates. Therefore, these data points were excluded from the dynamic measurement results, and the network properties at higher solids contents were therefore investigated using tensile testing methods (Fig. 4).

Frequency sweep tests further confirm the rigid network properties of the CNF suspension, which intensify with increasing solids content (Fig. 2(b)). The storage modulus (G') of the CNF suspension remained nearly constant across the measured frequency range and increased systematically with solids content. Furthermore, the complex viscosity exhibited pronounced shear-thinning-like behavior with increasing frequency (Fig. 2(c)). This indicates that while the complex viscosity was high at low frequencies, it decreased markedly as the frequency increased. This behavior persisted even at a solids content of 10%.

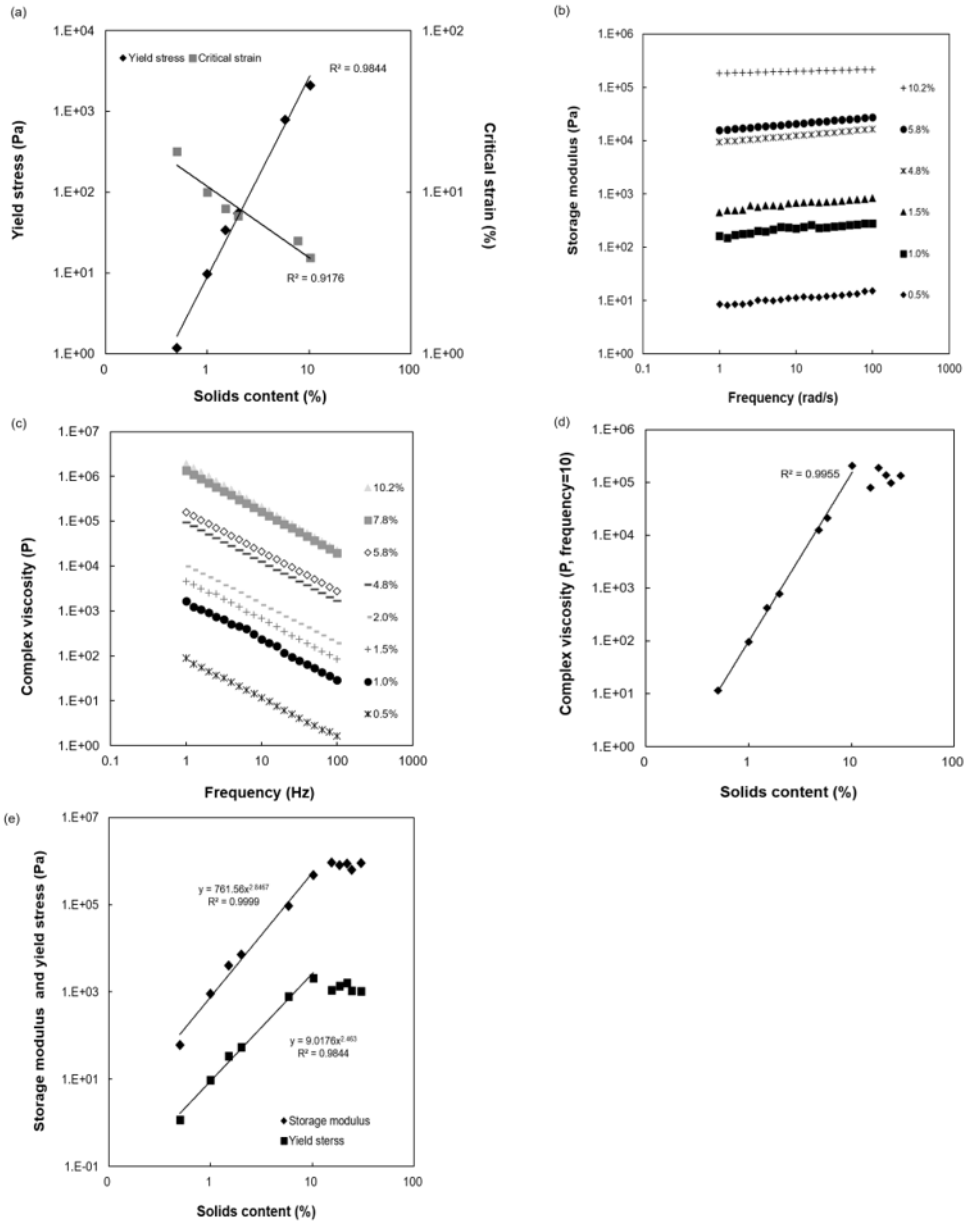

Fig. 2. Rheological properties of CNF suspension: (a) Yield stress and critical strain of CNF below the consistency of 10%, (b) Storage modulus of CNF suspension with change in frequency, (c) Viscosity of CNF suspension with change in frequency, (d) Viscosity of CNF suspension at the frequency of 10 Hz as the function of solids content, (e) Storage modulus and yield stress of CNF suspension as a function of solids content.

The relationship between complex viscosity and solids content at a fixed frequency of 10 Hz is shown in Fig. 2(d). Within the measurable range of the rheometer, the viscosity increased sharply with solids content, reflecting the progressive densification and entanglement of the nanofibril network. However, as the solids content exceeded this range, accurate measurements became increasingly difficult because the suspension gradually lost its fluid-like characteristics and exhibited substantial wall slip within the parallel-plate geometry. In addition, as discussed by Hubbe *et al.* (2017), rheological measurements of highly structured nanocellulose systems may be influenced by both wall-slip effects and slippage between partially fractured flocculated network fragments.

Within the accessible low-solids regime, both the storage modulus and the rheology-based yield stress followed power-law-type scaling with solids content (Fig. 2(e)). These trends describe the local scaling behavior of the CNF network under dynamic conditions. Beyond approximately 10% solids content, the CNF transitioned into a mat-like state that was too stiff for reliable dynamic measurements, leading to inconsistent results due to interfacial slip between the plates.

Mechanical Properties of CNF Mats at High Solids Contents

The morphology of the fibers was modified by increasing the number of passes through the grinder, thereby enhancing the degree of fibrillation. To evaluate the impact of these morphological changes, the tensile properties of CNF mats were measured across various solids contents and pass numbers. Stress-strain curves of CNF mat (99%) with increasing number of passes are shown in Fig. 3 (a). As the number of passes increased, both the tensile breaking stress and the strain at break improved significantly. While the pulp fiber mat (0 pass) exhibited brittle failure at low stress, the CNF mats (5 to 15 passes) showed much higher toughness and ductility.

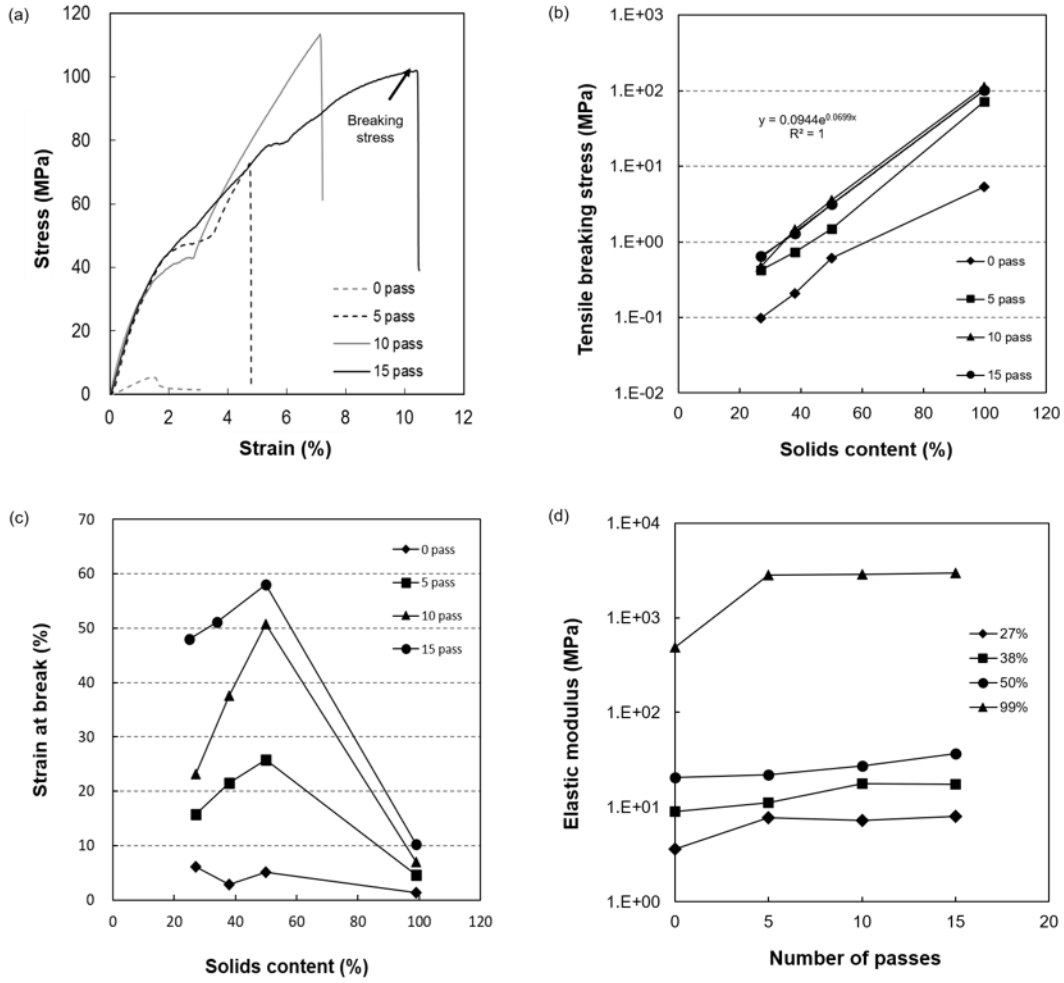

Fig. 3. Tensile properties of CNF mats: (a) Stress-strain curves of CNF mat (99%) with increasing number of passes, (b) Tensile breaking stress of CNF mats with increasing solids content, (c) Strain at break with increasing solids content, (d) Elastic modulus of the mat with increase in number of passes.

The relationship between tensile breaking stress and solids content is further analyzed in Fig. 3 (b). For all samples, the tensile breaking stress increased exponentially with solids content, a trend consistent with previous findings for pulp fibers (Belle and Odermatt 2016). Notably, as nanofibrillation progressed (increasing passes), the experimental data fit the ideal exponential function more closely ($R^2 \approx 1$). This improved fit is attributed to the increased network density and more uniform water distribution within the CNF mat resulting from progressive fibrillation. Furthermore, the wet strength of the CNF mats showed a remarkable improvement. At 50% solids content, the pulp fiber mat (0 pass) exhibited a tensile strength comparable to that of fully fibrillated CNF (15 passes) at only 25% solids content. The relatively high wet strength of CNF mats at lower solids content may be attributed to their large specific surface area, which allows water to be retained in a bound state rather than as free water. This enhances capillary forces within the fibrillar network, contributing to the development of network strength even at lower solids content. This suggests that nanofibrillation can compensate for lower solids content in terms of mechanical integrity, which is critical for improving runnability in papermaking processes.

Strain at break of pulp fiber (0 pass) generally decreased as solids content increased, as shown in Fig. 3 (c). In contrast, as the nanofibrillation progressed, the strain at break of fiber mats increased with solids content up to approximately 50%, followed by a rapid decrease. The initial increase is likely due to the enhanced inter-fibrillar contact area and friction as the network consolidates. However, above 50% solids content, intensified capillary forces arising from further water removal draw nanofibrils into close contact, leading to a highly densified structure. This densification, combined with increased inter-fibrillar interactions including hydrogen bonding, imposes strong constraints on molecular mobility, resulting in decreased plasticity and lower breaking strain.

Figure 3 (d) illustrates the change in the elastic modulus as a function of the number of passes. The elastic modulus of the mat increased with the number of passes. Nanofibrillation had a more pronounced effect on the dry state than on the wet state. While the wet CNF mats showed a 1.8 to 2.2-fold increase in elastic modulus compared to the wet pulp fiber mats (0 pass), the dry CNF mat (99% solids content, 15 passes) exhibited a 6-fold increase, reaching approximately 3 GPa. This rapid increase of the elastic modulus at high solids content is primarily driven by the transition from a friction-dominated network to a hydrogen-bonded consolidated structure, which also causes the decrease in the strain at break.

Unified Scaling of Network Strength of CNF Across the Entire Solids Content Range

The power-law relationship between solids content and network strength remained remarkably consistent across the entire measured range, regardless of whether dynamic rheometry or tensile testing was employed (Fig. 4(a)). In the tensile measurements, the tensile breaking stress was defined as the stress at which the consolidated CNF network began to fail irreversibly, thereby providing a practical counterpart to the yield point obtained from oscillatory rheology at lower solids contents. Although these two measures correspond to different mechanical events (onset of yielding *vs.* ultimate fracture), both reflect the integrity and load-bearing capacity of the CNF network under their respective testing conditions. Importantly, the governing network structure remains continuous across regimes, even though different mechanical properties are measured. Across the entire range from 0.5% to 99% solids content, all data points aligned along a single regression line on

a log–log scale. The coefficient in this power-law relationship is typically determined by the intrinsic characteristics of the fibers, such as aspect ratio, flexibility, and length (Tatsumi and Matsumoto 2007). However, the exponent is primarily governed by the network topology, particularly flocculation and the fractal organization of the fiber network, rather than solely by the aspect ratio of individual fibrils. In this study, the exponent was found to be 2.74. Despite the significantly higher aspect ratio of CNF compared to conventional pulp fibers, the observed exponent remains similar. This suggests that, at the network scale, CNF forms aggregated and entangled structures that behave as flocculated fiber networks, effectively masking the intrinsic nanoscale geometry of individual fibrils. Therefore, while intrinsic fiber characteristics may influence the magnitude of network strength, the scaling exponent reflects the hierarchical organization and connectivity of the network structure. Based on the experimental exponent of 2.74, the fractal dimension (DF) was calculated to be 1.4, which is in close agreement with the findings of Pääkkö *et al.* (2007).

A previous study on CNF flocculation (Saarikoski *et al*. 2012) suggested that CNF behavior is similar to pulp fibers, despite their vast dimensional differences. In this study, the power-law exponent relating network strength to solids content remained close to 3 across the entire measured range (0.5 to 99%). Tatsumi *et al*. (2002) demonstrated that the suspension network strength of cellulose fiber is logarithmically proportional to the aspect ratio, while Seth (1995) reported that wet strength is proportional to fiber length and inversely proportional to fiber coarseness. Since coarseness is a function of fiber thickness, these findings collectively emphasize that fiber aspect ratio can influence network strength within limited concentration ranges reported in the literature. However, in the present study, the consistent scaling behavior observed across a wide solids content range suggests that network-level structural organization plays a more dominant role than the intrinsic geometry of individual fibrils.

In this study, the effect of solids content was investigated over a significantly wider range than in previous studies. These results demonstrate that the flocculation behavior of nanofibrillated cellulose is fundamentally similar to that of traditional pulp fiber although CNF has a much higher aspect ratio and significantly smaller dimensions. This structural similarity was confirmed to persist even in the range of high solids content. However, differences were observed; the tensile breaking stress of the CNF network was 5 to 20 times higher than that of pulp fiber at equivalent solids contents. This indicates that CNF establishes a robust, load-bearing network at much lower concentrations while providing vastly superior mechanical resistance compared to pulp fibers.

The elastic modulus of the CNF mat as a function of solids content was derived from the strain-stress curve. As shown in Fig. 4(b), the elastic modulus increased exponentially with solids content, exhibiting a strong correlation. These results are consistent with general observations that network strength increases markedly with the dryness (solids content) of a wet web (Belle and Odermatt 2016).

The presence of interstitial water between nanofibrils in the wet mat is maintained by the high density of hydroxyl groups on the CNF surfaces. As the solids content increases, these lubricating water layers progressively thin out. The growing rigidity and stiffness of the wet mat are primarily attributed to surface tension, mechanical contacts, and fibrillar entanglements. These factors collectively enhance the effective friction and viscosity at inter-fiber contacts (Seth *et al*. 1984; Page 1993; Seth 1995), thereby leading to the observed exponential increase in the elastic modulus.

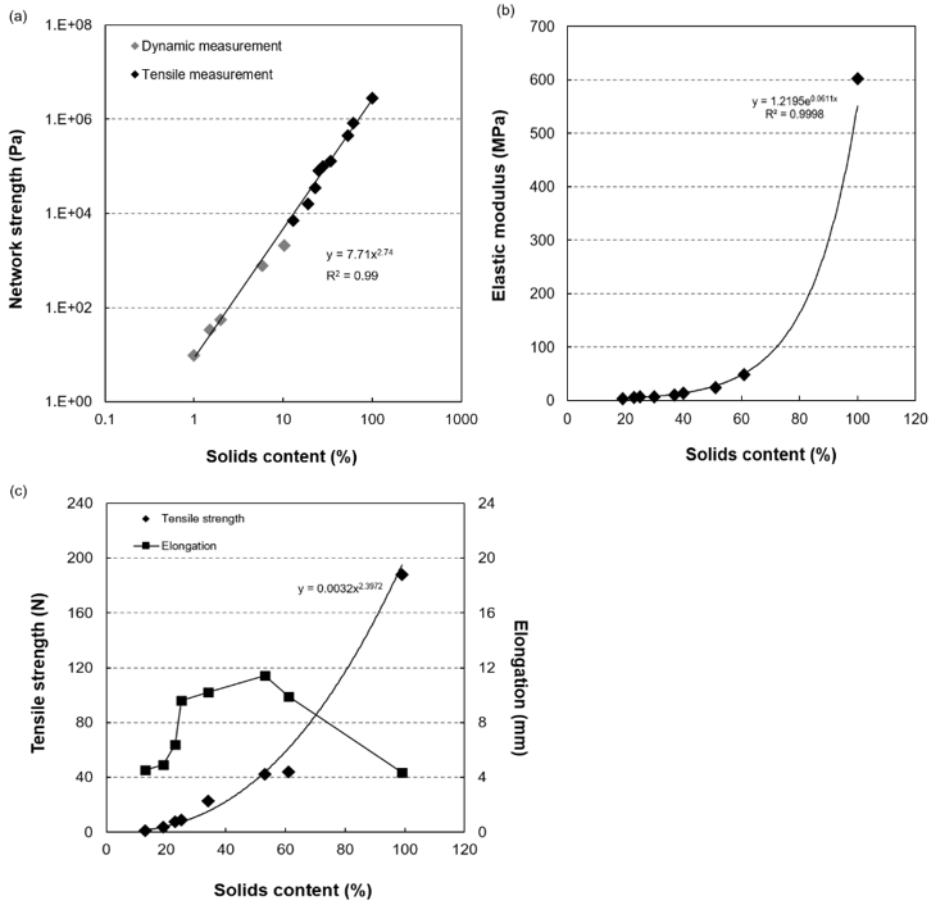

Fig. 4. Mechanical properties of 15 passes CNF mats; (a) Network strength of CNF mat with increasing solids content. CNF mat with solids content of 1 to 10% was measured with dynamic rheometer and CNF mat with solids content above 10% was measured with tensile tester, (b) Elastic modulus *vs.* solids content of CNF which was pressurized and dried wet mat, (c) Elongation and tensile strength of CNF wet mat with increasing solids content

Figure 4 (c) shows the tensile strength and elongation of the CNF mat as a function of solids content. Tensile strength consistently increased with solids content, exhibiting a notably sharp rise beyond approximately 50%. Interestingly, elongation showed a parabolic trend: it increased with solids content up to around 50%, then decreased above this threshold.

The steady increase in tensile strength is closely related to the interaction between nanofibrils. As water is removed, the decreasing distance between fibrils leads to a higher number of contact points. This phenomenon can be explained by the Laplace pressure mechanism as proposed by Campbell (1933). In a system where water exists between two surfaces, the negative curvature of the meniscus generates an attractive capillary force that pulls the surfaces together. According to Campbell's model, while the magnitude of this force remains constant as long as the meniscus exists at the edges, the evaporation of water continues to draw the fibrils into closer together. In a complex CNF matrix, these capillary forces act as powerful driving force for consolidation, increasing effectively as the interstitial spaces shrink and the fibrils are brought into intimate contact.

A critical inflection point in elongation was observed at approximately 50% solids content. Below this threshold, increases in tensile strength were accompanied by increases in elongation, suggesting that stress dissipation occurred primarily through fibrillar

rearrangement prior to failure. This behavior is consistent with general observations for wet paper and pulp fiber networks, where significant changes in viscoelastic response and network bonding dynamics occur in the intermediate solids content range (Hubbe *et al.* 2024). Such transitions have been attributed to the increasing contribution of hydrogen bonding and frictional contacts as water is progressively removed from inter-fiber and inter-fibrillar regions. In the present study, the elastic modulus similarly exhibited an exponential increase with solids content, with a noticeable change in slope occurring from approximately 40% solids content (Fig. 4(b)).

Furthermore, the results imply that a significant volume of water remains between nanofibrils even after pressing, up to the 50% threshold. The existence of this interstitial water suggests that the space it occupies could be potentially displaced by air or other media. This finding points to a potential strategy for controlling the pore size and distribution of CNF structures by adjusting the solids content during the consolidation process.

CONCLUSIONS

1. The mechanical and rheological properties of cellulose nanofibrils (CNF) were successfully integrated over an extensive range of solids contents from 0.5% to 99%. Across this entire spectrum, the network strength followed a consistent power-law relationship with a scaling exponent of 2.74, providing a comprehensive framework for understanding CNF consolidation from suspension to a dry mat.
2. The power-law exponent of 2.74 indicates that the flocculation behavior of nanofibrils is fundamentally similar to that of pulp fibers, despite the significantly higher aspect ratio and smaller dimensions of CNF, indicating that the observed power-law relationship is governed by network-level structural organization rather than the intrinsic geometry of individual fibrils.
3. The network strength of CNF was 5 to 20 times higher than that of conventional pulp fiber at equivalent concentrations, highlighting the significant role of enhanced inter-fibrillar interactions and effective contact area in CNF networks.
4. A CNF mat at a solids content of 25% exhibited a tensile breaking stress comparable to that of a pulp fiber mat at 50% solids content, indicating the superior consolidation efficiency of nanofibrillated cellulose networks, likely arising from increased surface-driven interactions such as capillary forces and hydrogen bonding.

ACKNOWLEDGMENTS

This work was supported by the National Research Foundation of Korea (NRF) grant funded by the Korea government (No. 2012011091).

Conflict of Interest

The authors declare that they have no known competing financial interests or personal relationships that could have appeared to influence the work reported in this paper.

REFERENCES CITED

Agoda-Tandjawa, G., Durand, S., Gaillard, C., Garnier, C., and Doublier, J. L. (2012). "Rheological behaviour and microstructure of microfibrillated cellulose suspensions/low-methoxyl pectin mixed systems. Effect of calcium ions," *Carbohydr. Polym.* 87(2), 1045-1057. https://doi.org/10.1016/j.carbpol.2011.08.021

Ai, Y., Liu, Y., Zhang, H., Wang, X., Li, J., and Chen, L. (2024). "Advances in cellulose nanomaterials for catalytic applications," *Science Bulletin*. 69(24), 3815-3819. https://doi.org/10.1016/j.scib.2024.06.013

Beghello, L. (1998). "Some factors that influence fiber flocculation," *Nord. Pulp Pap. Res. J.* 13(4), 274-279. https://doi.org/10.3183/npprj-1998-13-04-p274-279

Belle, J., and Odermatt, J. (2016). "Initial wet web strength of paper," *Cellulose* 23(4), 2249-2272. https://doi.org/10.1007/s10570-016-0961-7

Bennington, C. P. J., Kerekes, R. J., and Grace, J. R. (1990). "The yield stress of fiber suspensions," *Can. J. Chem. Eng.* 68(5), 748-757. https://doi.org/10.1002/cjce.5450680503

Björkman, U. (2000). *Flow of Flocculated Fibers*, 2nd Ed., TS Högskoletryckeriet, Stockholm, Sweden.

Björkman, U. (2003a). "Break-up of suspended fibre networks," *Nord. Pulp Pap. Res. J.* 18(1), 32-37. https://doi.org/10.3183/npprj-2003-18-01-p032-037

Björkman, U. (2003b). "Stress generation and transmission in suspended fibre networks," *Nord. Pulp Pap. Res. J.* 18(1), 38-43. https://doi.org/10.3183/npprj-2003-18-01-p038-043

Campbell, W. B. (1933). *The Cellulose-Water Relationship in Papermaking* (Forest Service Bulletin 84), Department of the Interior, Ottawa, Canada.

Cox, H. L. (1952). "The elasticity and strength of paper and other fibrous materials," *British Journal of Applied Physics* 3(3), 72-79. https://doi.org/10.1088/0508-3443/3/3/302

Hubbe, M. A., Tayeb, P., Joyce, M., Tyagi, P., Kehoe, M., Dimic-Misic, K., and Pal, L. (2017). "Rheology of nanocellulose-rich aqueous suspensions: A review," *BioResources* 12(4), 9556-9661. https://doi.org/10.15376/biores.12.4.Hubbe

Hubbe, M. A., Sjöstrand, B., Lestelius, M., Håkansson, H., Swerin, A., and Henriksson, G. (2024). "Swelling of cellulosic fibers in aqueous systems: A review of chemical and mechanistic factors," *BioResources* 19(3), 6859-6945. https://doi.org/10.15376/biores.19.3.Hubbe

Jones, J. L., and Marques, C. M. (1990). "Rigid polymer network models," *J. Phys. France* 51(11), 1113-1127. https://doi.org/10.1051/jphys:0199000510110111300

Karppinen, A., Saarinen, T., Salmela, J., Laukkanen, A., Nuopponen, M., and Seppälä, J. (2012). "Flocculation of microfibrillated cellulose in shear flow," *Cellulose* 19(6), 1807-1819. https://doi.org/10.1007/s10570-012-9766-5

Kerekes, R. J., Soszynski, R. M., and Tam Doo, P. A. (1985). "The flocculation of pulp fibres," in: *Papermaking Raw Materials*, V. Punton (ed.), Vol. 3, Mechanical Engineering Pub. Ltd., London, UK, pp. 265-310.

Kerekes, R. J., and Schell, C. J. (1992). "Characterization of fibre flocculation regimes by a crowding factor," *J. Pulp Paper Sci.* 18(1), J32-J38.

Kerekes, R. J. (2006). "Rheology of fibre suspensions in papermaking: An overview of recent research," *Nord. Pulp Pap. Res. J.* 21(5), 598-612. https://doi.org/10.3183/npprj-2006-21-05-p598-612

Kurath, S. F. (1959). "The network and viscoelastic properties of wet pulp (I): Dynamic mechanical properties," *Tappi J.* 42(12), 953-959.

Leitner, J., Hinterstoisser, B., Wastyn, M., Keckes, J., and Gindl, W. (2007). "Sugar beet cellulose nanofibril-reinforced composites," *Cellulose* 14(5), 419-425. https://doi.org/10.1007/s10570-007-9131-2

Lyne, L. M., and Gallay, W. (1954). "Fiber properties and fiber-water relationships in relation to the strength and rheology of wet webs," *Tappi J.* 37(12), 581-596.

Nordman, L., Nyblom, I., and Neimo, L. (1972). "IUPAC/EUCEPA Symposium on Man-made Polymers Papermaking Proceedings," Finnish Pulp and Paper Research Institute, Helsinki, Finland, pp. 257.

Pääkkö, M., Ankerfors, M., Kosonen, H., Nykänen, A., Ahola, S., Österberg, M., Ruokolainen, J., Laine, J., Larsson, P. T., Ikkala, O., and Lindström, T. (2007). "Enzymatic hydrolysis combined with mechanical shearing and high-pressure homogenization for nanoscale cellulose fibrils and strong gels," *Biomacromolecules* 8(6), 1934-1941. https://doi.org/10.1021/bm061215p

Page, D. H., El-Hosseiny, F., Winkler, K., and Lancaster, A. P. S. (1977). "Elastic modulus of single wood pulp fibers," *Tappi J.* 60(4), 114-117.

Page, D. H. (1993). "A quantitative theory of the strength of wet webs," *J. Pulp Paper Sci.* 19(4), J175-J176.

Saarikoski, E., Saarinen, T., Salmela, J., and Seppälä, J. (2012). "Flocculated flow of microfibrillated cellulose water suspensions: An imaging approach for characterisation of rheological behaviour," *Cellulose* 19(3), 647-659. https://doi.org/10.1007/s10570-012-9661-0

Seth, R. S., Page, D. H., Barbe, M. C., and Jordan, B. D. (1984). "The mechanism of the strength and extensibility of wet webs," *Svensk Papperstidn.* 87(6), R36-R43.

Seth, R. S. (1990). "The effect of fiber properties on wet web strength," *J. Pulp Paper Sci.* 16(4), J160-J165.

Seth, R. S. (1995). "The effect of fiber length and coarseness on the tensile-strength of wet webs - a statistical geometry explanation," *Tappi J.* 78(3), 99-102.

Siró, I., and Plackett, D. (2010). "Microfibrillated cellulose and new nanocomposite materials: A review," *Cellulose* 17(3), 459-494. https://doi.org/10.1007/s10570-010-9405-y

Solhi, L., Guccini, V., Heise, K., Solala, I., Niinivaara, E., Xu, W., Mihhels, K., Kröger, M., Meng, Z., Wohlert, J., Tao, H., Cranston, E. D., and Kontturi, E. (2023). "Understanding nanocellulose–water interactions: Turning a detriment into an asset," *Chem. Rev.* 123(5), 1925-2015. https://doi.org/10.1021/acs.chemrev.2c00611

Tatsumi, D., Ishioka, S., and Matsumoto, T. (2002). "Effect of fiber concentration and axial ratio on the rheological properties of cellulose fiber suspensions," *Nihon Reoroji Gakkaishi* 30(1), 27-32. https://doi.org/10.1678/rheology.30.27

Tatsumi, D., and Matsumoto, T. (2007). "Rheological properties of cellulose fiber wet webs," *J. Cent. South Univ. T.* 14(s1), 250-253.

Wågberg, L., and Nordqvist, T. (1999). "Detection of polymer induced flocculation of cellulosic fibres by image analysis," *Nord. Pulp Pap. Res. J.* 14(3), 247-255. https://doi.org/10.3183/npprj-1999-14-03-p247-255

Xu, J., Wang, P., Yuan, B., and Zhang, H. (2024). "Rheology of cellulose nanocrystal and nanofibril suspensions," *Carbohydrate Polymers* 324(13), article 120216. https://doi.org/10.1016/j.carbpol.2023.121527

Youn, H. J., and Lee, H. L. (2002). "An experimental investigation of the effect of pulp

types, mechanical treatments and crill contents on fibre network strength," *Nord. Pulp Pap. Res. J.* 17(2), 187-192. https://doi.org/10.3183/npprj-2002-17-02-p187-192

Zhang, R., Guo, J., Zhang, L., Wang, S., Chen, X., and Zhu, J. Y. (2023a). "Single-molecular insights into cellulose nanofibril assembly," *Nature Communications* 14, 1100. https://doi.org/10.1038/s41467-023-36856-8

Zhang, R., Hu, Z., Wang, Y., Hu, H., Li, F., Li, M., Liu, P., Wang, Y., Zhu, W., and Lu, J. (2023b). "High-density cellulose nanofibril assembly leads to upgraded enzymatic and chemical catalysis of fermentable sugars, cellulose nanocrystals and cellulase production by precisely engineering cellulose synthase complexes," *Green Chemistry* 25, 1096-1106. https://doi.org/10.1039/D2GC03744K

Zimmermann, T., Pöhler, E., and Geiger, T. (2004). "Cellulose fibrils for polymer reinforcement," *Adv. Eng. Mater.* 6(9), 754-761. https://doi.org/10.1002/adem.200400097

Article submitted: January 19, 2026; Peer review completed: March 21, 2026; Revised version received and accepted: May 29, 2026; Published: June 8, 2026.
DOI: 10.15376/biores.21.3.6726-6740